GRATINGS: THEORY AND NUMERIC APPLICATIONS

Tryfon Antonakakis
Fadi Baïda
Abderrahmane Belkhir
Kirill Cherednichenko
Shane Cooper
Richard Craster
Guillaume Demesy
John DeSanto
Gérard Granet
Boris Gralak
Sébastien Guenneau
Daniel Maystre
André Nicolet
Brian Stout
Fréderic Zolla
Benjamin Vial

Evgeny Popov, Editor

Institut Fresnel, Université d'Aix-Marseille, Marseille, France
Femto, Université de Franche-Compté, Besançon, France
Institut Pascal, Université Blaise Pascal, Clermont-Ferrand, France
Colorado School of Mines, Golden, USA
CERN, Geneva, Switzerland
Imperial College London, UK
Cardiff University, Cardiff, UK
Université Mouloud Mammeri, Tizi-Ouzou, Algeria

ISBN: 978-2-8539-9860-4

www.fresnel.fr/numerical-grating-book

ISBN: 978-2-8539-9860-4

First Edition, 2012, Presses universitaires de Provence (PUP)

World Wide Web:

www.fresnel.fr/numerical-grating-book

Institut Fresnel, Université d'Aix-Marseille, CNRS
Faculté Saint Jérôme,
13397 Marseille Cedex 20,
France

Gratings: Theory and Numeric Applications, Evgeny Popov, editor (Institut Fresnel, CNRS, AMU, 2012)

Chapter 1:

Introduction to Diffraction Gratings: Summary of Applications

Evgeny Popov

Table of Contents:

Chapter 1

Introduction to Diffraction Gratings: Summary of Applications

Evgeny Popov

Institut Fresnel, CNRS, Aix-Marseille University, Ecole Centrale Marseille, Campus de Saint Jerome,13013 Marseille, France
e.popov@fresnel.fr www.fresnel.fr/perso/popov

Periodic systems play an important role in science and technology. Moreover, desire for order in Nature and human society has accompanied development of philosophy. Simple periodical oscillation is referenced as 'harmonic' in mechanics, optics, music, etc., the name deriving from the Greek *ἁρμονία* (harmonía), meaning "joint, agreement, concord" [1.1]. It is not our purpose here to study harmony in general, nor harmony in physics. We are aiming to much more modest target: rigorous methods of modeling light propagation and diffraction by periodic media.

The methods presented in the book have already shown their validity and use from x-ray domain to MW region, for nonmagnetic and magnetic materials, metals and dielectrics, linear and nonlinear optical effects. The existing variety of these methods is due not only to historical reasons, but mainly to the absence of The Method, a universal approach that could solve all diffraction problems. Some of the approaches cover greater domain of problems, but more specialized ones are generally more efficient. The other reason of the great number of methods is the complexity and variety of their objects and applications.

1.1. Diffraction property of periodic media

The most important property of diffraction grating to create diffraction orders has been documented by Rittenhause for the first time in 1786 [1.2] due to the observation made by Francis Hopkinson through a silk handkerchief. The appearance of diffraction orders rather than the specularly reflected and transmitted beams was studied experimentally by Young in 1803 [1.3] with his discovery of the sine rule. A detailed presentation of the analytic properties of gratings can be found in Chapter 2.

Secondary-school pupils are supposed nowadays to know the Snell-Descartes law, which undergraduate students in universities are supposed to be able to demonstrate: single-ray diffraction on a plane interface results in a single transmitted and single reflected rays. The critical advantage of periodic perturbation of the interface (variation of the refractive index or surface corrugation) changes the impulsion (wavevector surface component $\vec{k}_{S,m}$) of the incident wave $\vec{k}_{S,i}$ along the surface by adding or subtracting an integer number of grating impulses (grating vectors) $\vec{K}$:

$$\vec{k}_{S,m} = \vec{k}_{S,i} + m\vec{K} \tag{1.1}$$

where $\vec{K} = \frac{2\pi}{d}\hat{d}$ and d is the grating period in a unit-vector direction $\hat{d}$.

If the interface lies in the xy-plane and the periodicity is along the x-axis (Fig.1.1), and the incidence lies in a plane perpendicular to the grooves, the equation in reflection takes the form of the so-called *grating equation*:

$$\sin\theta_m = \sin\theta_i + m\frac{\lambda}{d} \tag{1.2}$$

where λ is the wavelength of light.

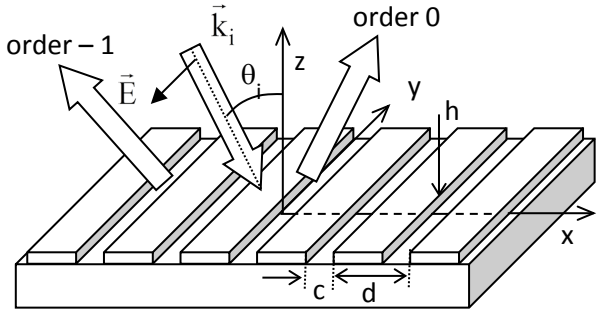

Fig.1.1. Lamellar grating working in in-plane regime in TM (transverse magnetic) polarization, together with the coordinate system, incident wavevector.

The case of conical (off-plane) diffraction by a plane grating having one-dimensional periodicity can also be described by eq.(1.1), preserving the wavevector component parallel to the groove direction:

$$\begin{aligned} k_{y,m} &= k_{y,i} \\ k_{x,m} &= k_{x,i} + mK \\ k_{z,m} &= \sqrt{k^2 - k_{x,m}^2 - k_{y,i}^2} \end{aligned} \tag{1.3}$$

where k is the wavenumber in the cladding. As a result, the diffracted beams lie on a cone, thus the name *conical diffraction*.

Two-dimensional periodicity (having grating vectors $\vec{K}_1$ and $\vec{K}_2$) imposed on the optogeometrical properties of the plane interface creates two sets of diffraction orders together with their spatial combinations, subjected to the same rule formulated just before eq.(1.1):

$$\vec{k}_{S,mn} = \vec{k}_{S,i} + m\vec{K}_1 + n\vec{K}_2 \tag{1.4}$$

Pure three-dimensional (3D) periodicity appears in crystallography and photonic crystals, if the substance is assumed to fill the entire space. The third-direction periodicity imposes additional condition to the wavenumber (said more precisely, to $k_{z,m}$, which is already defined by the wave equation as given in the third equation of (1.3)), which leads to creation of discrete modes propagating in 3D periodic structures. This also leads to the appearance of propagating and forbidden zones structure.

1.2. Classical gratings in spectroscopy

The most common application of diffraction gratings is due to the fact that outside of the specular order (m = 0), the diffraction order direction depends on the wavelength, as stated in eq.(1.2). The result is that the grating acts as a dispersive optical component, with several advantages when compared to the prisms:

1. The grating can be a plane device, while the prism is a bulk one that requires larger volumes of optically pure glass (to add the difficulties of weight and temperature expansion constrains).
2. Provided a suitable reflecting material, the grating can work in spectral regions, where there is no transparent 'glass' with sufficient dispersion.
3. Grating dispersion can be varied, as it depends on the groove period, while prism dispersion depends on the material choice and groove angle, which gives quite limited choices.

Since the first works of Young, followed by Fraunhofer's quite serious attention to diffraction gratings use and properties [1.4], there is rarely more important device in spectroscopy achievements that lay the basis of modern physics. An interested reader can find some important aspects of their history, properties, and application in [1.5]. Despite the above-listed advantages compared to prisms, the diffraction gratings never have sufficient performance for their spectroscopy customers:

1. *There is no enough diffraction efficiency*, defined as the ratio of the incident light diffracted in the order used by the application.

This is probably the problem that has been mostly treated by rigorous grating methods, because they are the only ones to provide feasible results on the energy distribution, while the other characteristics (spectral resolution, scatter, dispersion, order overlap, etc.) can be obtained by simpler approaches.

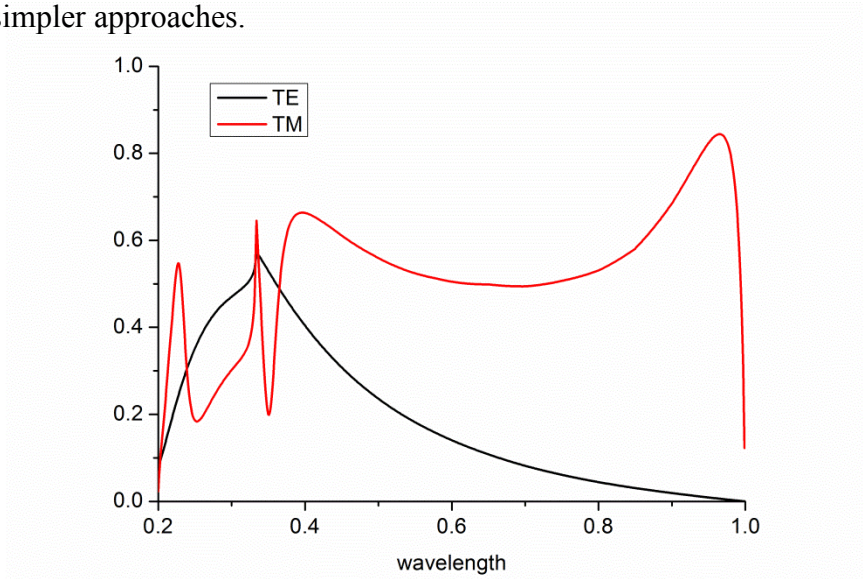

Fig.1.2. Diffraction efficiency of aluminum-made sinusoidal grating with period d = 0.5 μm as a function of the wavelength. Littrow mount (–1st order diffracted in the direction of the incident beam) for the two fundamental polarizations (transverse electric TE and transverse magnetic TM).

A typical spectral dependence of the diffraction efficiency (defined more precisely as the ratio between the energy flow in the corresponding order and the energy flow in the incident order in z-direction) of a surface-relief sinusoidal grating made of aluminum and working in the -1^{st} Littrow mount[1] is presented in Fig.1.2. As observed, the problems of spectral variation of efficiency adds to its polarization dependence.

2. *There is no enough resolution,* defined as the ratio between the working wavelength and the smallest distinguishable (as usual, defined using the Rayleigh criterion) spectral interval:

[1] Littrow mount means retrodiffusion, when the diffracted beams propagates in a direction opposite to the incident beam, i.e. $\sin\theta_{-1} = -\sin\theta_i$

$$R = \frac{\lambda}{\Delta\lambda} \tag{1.5}$$

Classical diffraction theories show that the spectral resolution is proportional to the number of grooves illuminated by the incident beam, and inversely proportional to $\cos(\theta_i)$, if we consider 1D periodicity in non-conical diffraction (speaking more precisely, the inverse proportionality implies to the sum of the cosines of the incident and the diffracted angles). The latter dependence gives advantages to grazing incidence for higher spectral resolution applications, namely astronomy.

3. *The efficiency depends on the polarization.*

Laser resonators usually use Brewster windows, so that the requirements are for high-efficient grating working in TM (transverse magnetic) polarization. However, spectroscopic applications do not like this at all. In astronomy, this property can be quite costly, because the loss of a half of the incident light intensity requires twice the exposer time. Low polarization dependent losses (PDL) are one of the most important criterions in optical communications, in general, and in grating applications for wavelength demultiplexing, in particular, necessary for multichannel optical connections. Fortunately, contrary to stellar spectroscopy, gratings used in optical communications work in only very small spectral interval, and are used in quite smaller sizes, so that there exist several solutions that provide high efficiency in unpolarized light over a limited spectral region. The idea is to shift the maxima in the spectral dependence of the two polarizations in Fig.1.2 in order to make them overlap at some required wavelength. One solution is to use a grating having two-dimensional (2D) periodicity, as shown further on in Fig.7.1. The period in the perpendicular direction is sufficiently small as not to introduce additional diffraction orders, and this additional corrugation can shift the position of the TE maximum to longer wavelengths [1.6].

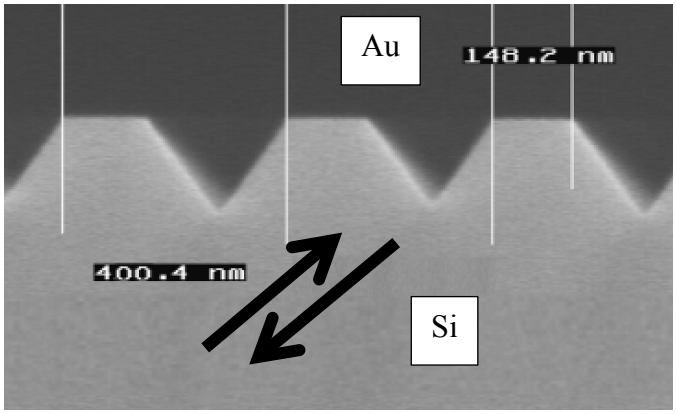

Fig.1.3. SEM picture of the profile of a grating etched in Si wafer and used for wavelength demutiplexing (after [1.7], with the publisher's permission)

Another more conventional solution is to use a classical grating with a 1D periodicity, but having a deformed profile in order to perform the same shift of the TE maximum [1.7, 8]. This can be achieved by introducing a flat region at the bottom of the grooves and "sharpening" the groove triangle, which needs a sharper apex angle. While this is quite difficult to be made with grating ruling or holographic recording, etching in crystalline silicon naturally produces grooves with 70.5° apex angle, as observed in Fig.1.3. A flat region on the top is made if the etching is not complete. When covered with gold, such grating can be used from the silicon side, which is transparent at wavelengths around 1.55 μm. Unpolarized

efficiency greater than 80% can be kept over the communication interval of 50-60 nm, as observed in Fig.1.4.

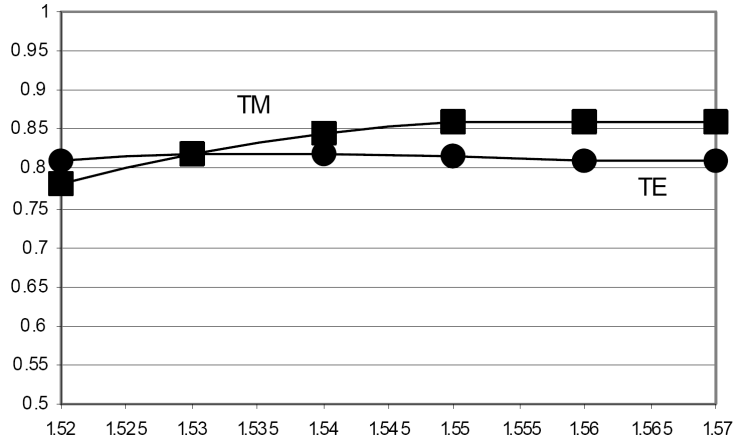

Fig.1.4. Spectral dependence of efficiency in -1st order for the grating shown in Fig.1.3 (after [1.7] , with the publisher's permission).

4. *There is an overlap of diffraction orders.*

As stated by the grating equation, if the period is chosen to provide diffraction orders inside a large spectral interval, the second diffracted order has the same direction of propagation as the first one for wavelength of light twice shorter. This problem is avoided in many spectroscopic devices by three different methods: additional spectral filtering of undesired orders; interchange of grating having different spatial frequency (period); adding cross-dispersion grating for echelle applications.

In addition, there is a contradiction between some requirements as, for example, free spectral range (spectrum covered by the grating), dispersion and overlap of orders. In some cases, the only compromise is to use interchangeable gratings in order to cover larger spectral range without order overlap and maintaining higher dispersion. Some spectrographs are designed having multiple channels with splitting of the incident beam between them, however reducing the illumination power in each channel.

1.3. Echelle gratings in astronomy

In astronomy, measurements of very low signals coming from far cosmic objects require large periods of time, so that the loss of energy due to low efficiency or/and strong polarization dependence leads to a further growth of costs. When efficiency constraints are added to the independence of the polarization, the only known solution is the echelle grating (high groove-angle triangular groove profile used in grazing incidence, Fig.1.5) that has the advantages of almost equal and high efficiency in both fundamental polarizations [1.9].

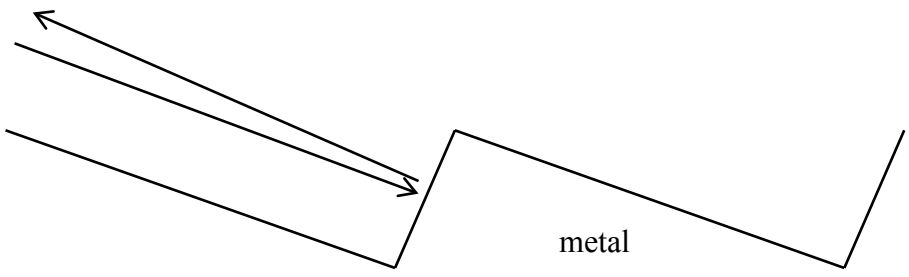

Fig.1.5. Schematical presentation of echelle grating.

The high efficiency in unpolarized light is obtained when the diffraction is made as if light is reflected by the working facet in its normal direction. Of course, it is necessary that the reflections at consecutive facets are in phase. The problem is that the efficiency varies rapidly with the wavelength, and the maxima switch between consecutive orders (Fig.1.6). The separation of orders is usually made using another shorter-period grating with grooves perpendicular to the echelle (called cross-dispersion), so that the different orders are separated in direction perpendicular to the echelle dispersion direction.

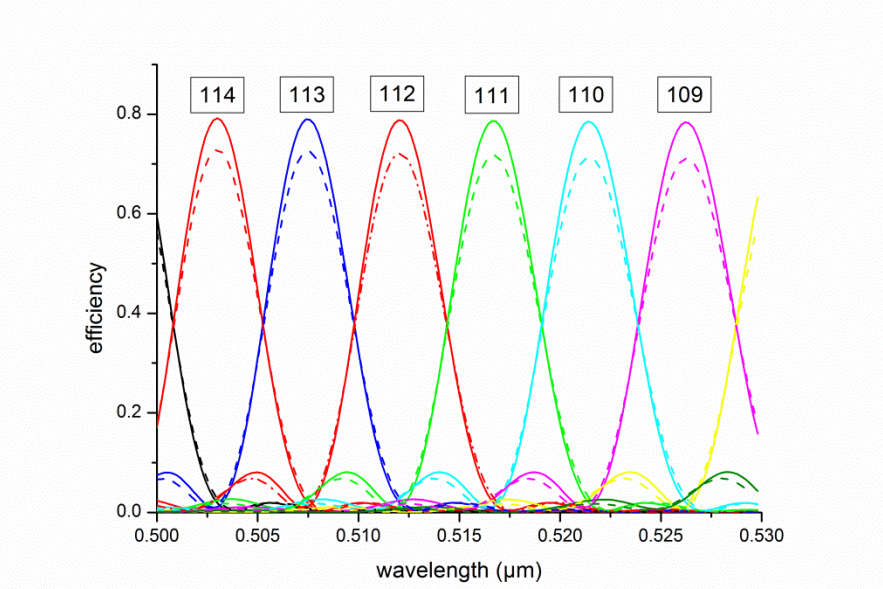

Fig.1.6. Diffraction efficiency of an echelle made of aluminum with 31.6 grooves/mm and 64° groove angle of the working facet. Incident angle is equal to 64°. The numbers of the diffraction orders are indicated in the figure.

Echelle gratings are also used in transmission, glued to the hypotenuse face of a prism that has a role to deviate back the beam diffracted by the grating, so that the principal diffracted order of the device propagates almost in the same direction as the incident beam for a chosen central wavelength. The device is known as a Carpenter prism or GRISM and gives the possibility to convert an imaging device (camera) into a long slit spectrograph [1.10], commonly used in airborne or space borne scientific missions.

UV excimer lasers used in photolithography at 193.3 nm wavelength can be equipped with an echelle grating for narrowing the spectral line. While in lasers working in the visible and IR, the resonators are equipped with diffraction gratings with symmetrical grooves working in -1^{st} order than easily can be made holographically or lithographically, a grating working in the lowest order at 193.3 nm must have more than 9 000 gr/mm, very difficult for fabrication and impossible for replication. Echelles take longer to be made and are more expensive as they require mechanical ruling engines with temperature control and clean environment, but have large periods and can be replicated from the ruled masters and submasters to become available at acceptable prices.

1.4. Gratings as optical filters

Spectroscopic applications of gratings use one or more diffraction orders that differ from the specular reflected and transmitted ones, because of the required spectral dependence. There exist, however, several applications that use the zero order(s), even with corrugation of the

surface or modulation of the refractive index in the grating region. These are devices having refractive or reflection properties in the zeroth order that are modified by the grating surface.

1.4.1. Zero-order diffraction (ZOD) imaging

One of the applications uses the diffraction in higher orders to change the spectral dependency in the zero order, as light that is diffracted in the higher order(s) is absent in the zero order. The structure known as zero-order diffraction *(ZOD)* microimage [1.11] represents a transmission grating (usually with a rectangular or triangular groove form that can be replicated by relief printing in plastic sheet. Appropriately choosing the groove depth, one obtains broad-band color filters in transmission by using non-absorbing materials without colorants that can bleach.

Another type of gratings have periods, smaller than the wavelength in the substrate and the cladding, chosen to avoid the propagation of other that the zero orders. Such structures are known as *subwavelength gratings*, and they play important role in integrated optical devices and recently in plasmonics to transfer energy from one to another guided mode in dielectric or metallic waveguides, or to change the mode direction, or to focus guided light (see Section 1.5).

1.4.2. Surface/guided mode excitation

A subwavelength grating can serve to couple the incident light to surface or cavity resonances that can exist in the grating structure. The absence of higher orders means only that they are evanescent rather than propagating in the cladding or in the substrate. The horizontal component of their propagation constant (say, k_x) is larger than the wavenumber in the surrounding media, and thus it can excite a surface or waveguide mode that is subjected to the same requirement in order to stay confined to the surface. The grating action is the same as in the coupling between the incident wave and one of the diffraction orders, only that now $k_{x,-1}$ is equal to the real part of the mode propagation constant k_g:

$$\mathrm{Re}(k_g) = k_{x,i} - K \tag{1.6}$$

To fail to see the quite small difference between k_g and k_0 in the case of surface plasmons on highly conducting metal surfaces is one of the rare failures of Lord Rayleigh [1.12] when trying to explain Wood's anomalies [1.13]. The case when $k_{x,m} = k_0$ represents a transition of the m-th diffracted order between a propagating and an evanescent type, as follows from eq.(1.3). This transition leads to a redistribution of energy between the propagating orders, observed in efficiency behavior as a phenomenon called cut-off anomaly.

Lord Rayleigh attributed Wood's anomalies to the cut-off of higher orders, whereas the true explanation is that Wood anomaly is due to surface plasmon excitation. It is easy to judge nowadays, but the difference in the spectral and angular positions of the cut-off and surface plasmon anomaly sometimes is smaller than the experimental error, or more important, the error in the knowledge of the grating period. The resonant nature of the surface-plasmon anomaly has much more pronounced features than the cut-off anomaly, a fact first noticed by Fano [1.14] and further developed by Hessel and Oliner [1.15]. The form of the so-called Fano-type anomaly can easily be derived from the interference with a non-resonant contribution (for example, non-resonant reflection by the grating layer) and a resonant effect (for example, excitation by the incident wave of a surface mode that is diffracted back into the direction of the non-resonant wave), as sketched in Fig.1.7.

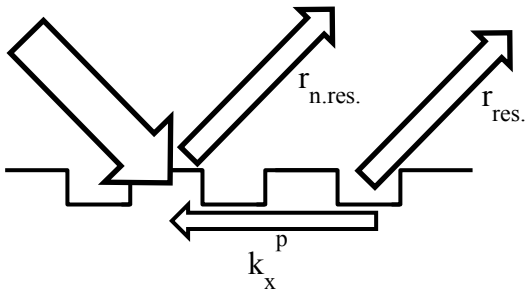

Fig.1.7. Process of interference between the non-resonant and the resonant reflections (second term in eq.(1.7)) that is created due to the excitation of the surface or guided wave through the –1st grating order, and then radiated into the cladding through the +1st diffraction order.

Here, by mode, we mean a surface or guided wave that represents an eigen (proper) solution of the homogeneous diffraction problem (assuming non-zero diffracted field without incident wave). The latter effect is commonly described in physics as having a Lorentzian character (e.g. electric circuit dipole oscillator). For example, the wavelength dependence of the total reflectivity r will be the sum of the non-resonant and the resonant Lorentzian contributions:

$$r = r_{n.res.} + \frac{c_{res.}}{k_{x,i} - k_x^p} \tag{1.7}$$

where the coefficients $r_{n.res.}$ and $c_{res.}$ are slowly varying functions of the incident wave parameters. The pole k_x^p of the resonant term is equal to the surface/guided wave propagation constant. The Fano-type equation is obtained by taking the common denominator in eq.(1.7):

$$r = r_{n.res.} \frac{k_{x,i} - k_x^z}{k_{x,i} - k_x^p} \tag{1.8}$$

with $k_x^z = k_x^p - c_{res.}/r_{n.res.}$ representing a zero of the reflectivity. The formula implies that for each resonance, there exist an associated zero, that is expressed as a minimum of the anomaly. In reality, the pole has always non-zero imaginary part due to the interaction between the incident and the surface/guided wave. The zero takes, in general, complex values, but there are several important practically cases when the zero could become (and remains) real, i.e., the reflectivity can become zero. The imaginary part of the pole determines the quality factor (width) of the resonant maximum.

The same reasoning applies in transmission (and in any other existing propagating order), with the same pole (same resonance), but different zeros. Depending on the imaginary parts of the pole and the zero, sometimes the resonant anomaly can show itself as a Lorentzian maximum, sometimes as a pure minimum on otherwise highly-reflecting background, sometimes both maximum and minimum can manifest themselves. The important cases when the zeros are almost real are used in surface plasmon absorption detectors and in resonant dielectric grating filters (see the next two subsections).

1.4.3. Surface plasmon absorption detector

Wood anomaly can sometimes lead to a total absorption of light by shallow metallic gratings with groove depth that does not exceed 10% of the wavelength. This phenomenon was called *Brewster effect* in metallic gratings [1.16] and has found an important application in chemical

and biochemical surface-plasmon grating detectors [1.17]. The effect of total light absorption appears in a narrow spectral and angular interval (Fig.1.8).

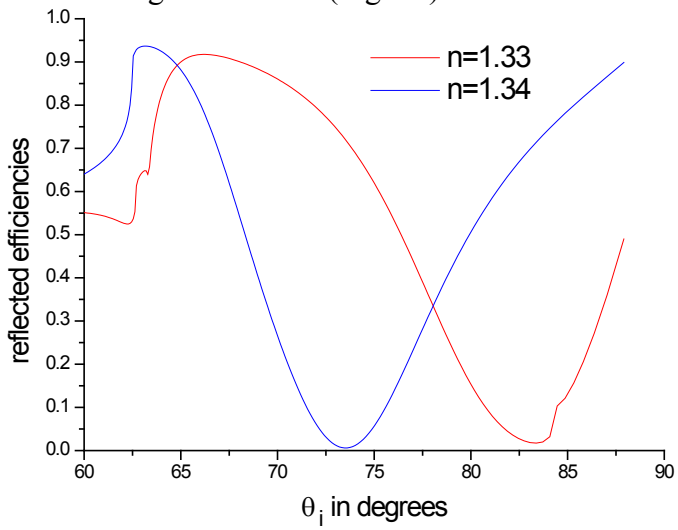

Fig.1.8. Reflectivity of an optical surface plasmon detector as a function of the incident angle. Wavelength equals 850 nm, TM polarization. Cladding is glass, the substrate index for the two curves is indicated in the figure, and the grating layer is made of silver with thickness of 40 nm. The grating profile function contains two Fourier harmonics: $35\sin(2\pi x/d)+59\sin(4\pi x/d+\pi/2)$ *with the depths given in nanometers (after [1.18], with the permission of the publisher).*

The position of the anomaly depends on the propagation constant of the plasmon surface wave that is quite sensible to the variation of the refractive index of the surrounding dielectric, thus the determination of the position of the anomaly brings information about the composition of the surrounding medium, i.e., serves as an optical detector (Fig.1.8). Introduction of the second Fourier component of the profile function increases the direct interaction between the plasmon surface waves propagating in opposite directions (the grating vector of the second harmonic is twice longer that of the first one), interaction that increases the sensitivity of the device.

1.4.4. Resonant dielectric filters

There is a particular case when the maximum in the reflectivity due to the resonant waveguide mode excitation stays theoretically at 100% on a low-reflective non-resonant background value. This is the case of corrugated dielectric waveguides having symmetrical grooves. If, in addition, the substrate is identical to the cladding, the zero in reflection remains real whatever the other parameters, i.e. a 100% maximum is accompanied by a 0 value minimum in the reflectivity (Fig.1.9). This peculiarity was accidentally found in 1983 [1.19, 20] followed by a theoretical explication in 1984 [1.21]. The effect has been independently rediscovered in 1989 by Magnusson [1.22], who has done a lot for its analysis, and quite important practically, for its extension in transmission [1.23]. The advantage of the device is that the quality factor increases with the decrease of the groove depth, i.e. very narrow-line spectral filters can be obtained using shallow gratings, at least theoretically. However, as usual, the advantage is paid back somewhere, namely in the tight angular tolerances: when eq.(1.6) results in high spectral sensibility, it also is responsible for strong angular sensibility. Sentenac and Fehrembach [1.24] proposed to introduce a direct coupling between the waveguide modes propagating in the opposite direction (as was done in Fig.1.8), but this time aiming to a significant *reduction* of the angular sensibility of the effect.

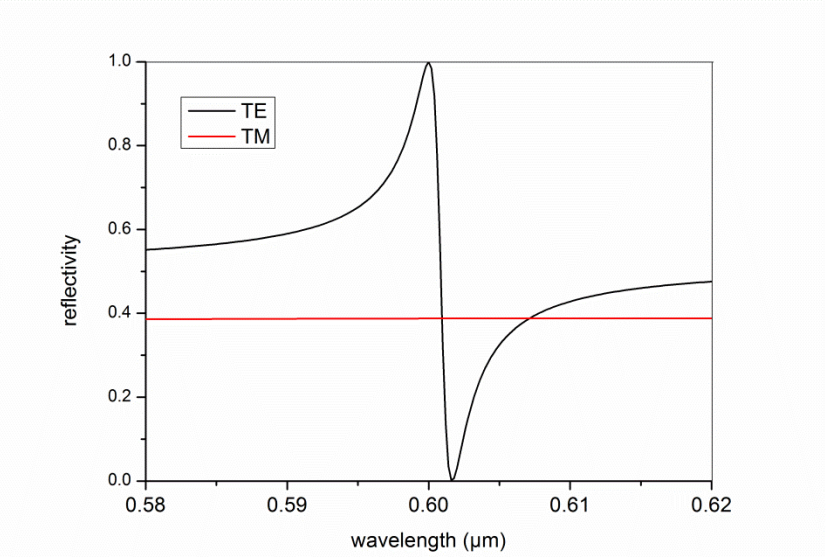

Fig.1.9. Reflection by a corrugated dielectric waveguide. Symmetrical triangular profile with groove angle equal to 10°. Substrate and cladding have optical index equal to1, the layer has index 2.3 and its thickness is equal to 69 nm. Incident angle is equal to 26.7°. Excitation of TE waveguide mode leads to a narrow spectral anomaly.

The idea was based on the flattening of the angular dependence of the guided wave propagation constant on the boundaries of the forbidden gaps, created by the direct mode coupling due to the structure periodicity, one of the basic properties of photonic (and electronic) crystals.

1.4.5. Enhanced transmission through hole arrays in metallic screens

In 1998 Ebbesen et al. [1.25] reported an interesting effect on metallic screen perforated with circular holes (Fig.1.10a). They were surprised to observe peaks with relatively strong transmission in the spectral dependence (Fig.1.11).

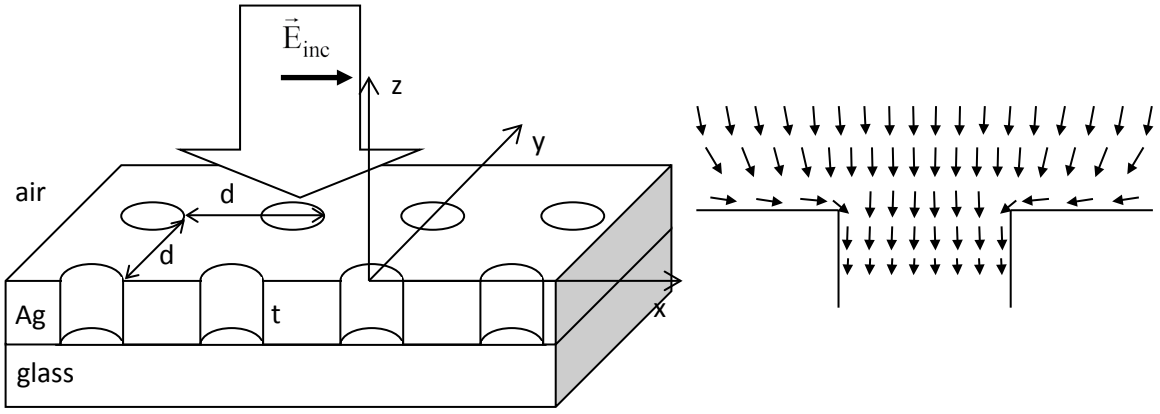

Fig.1.10. (a) Schematical representation and notations of a two-dimensional hole array perforated in a metallic screen deposited on a glass substrate and illuminated from above with linearly polarized incident wave. (b) Surface-plasmon assisted energy flow inside the aperture close to the resonance.

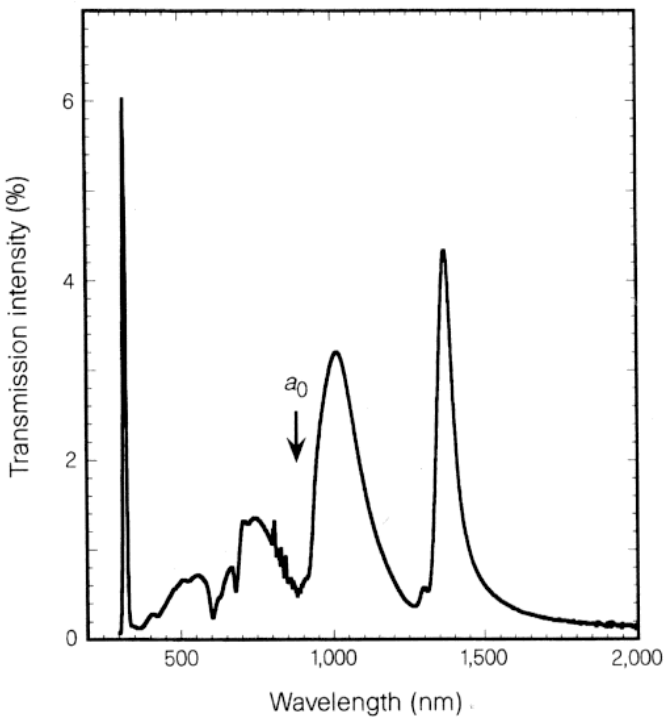

Fig.1.11. Spectral dependence of the transmission of the structure presented in Fig.1.10a, with d = 0.9 μm, t = 0.2 μm, and hole diameter of 0.2 μm (after [1.25], with the publisher's permission).

These peaks were identified as resulting from surface plasmon excitation on the upper, or the lower surface. Many theoretical and experimental works appeared as a result of this discovery, which revived the interest to surface plasmons and grating structure, leading to a new name of the plasmon studies called now *plasmonics*.

It seems nowadays that the explanation of the enhanced transmission observed in Fig.1.11 lies in the common action of two phenomena [1.26]. The first one is the surface plasmon excitation that enhances the electromagnetic field intensity near the entrance apertures, as represented schematically in Fig.1.10b. The second phenomenon is the tunneling of the mode in the vertical hollow waveguides inside the holes. Although for small holes even the lowest mode is evanescent (contrary to 1D lamellar gratings, where TEM mode exists without cut-off), it gives the possibility of energy transfer from the upper to the lower interface, much more efficiently than the tunneling through the non-perforated screen [1.27].

One unexpected consequence of the observation of Ebbesen et al. came in fluorescence single-molecule microscopy and in the biomembrane studies. Both require small measuring volumes in order to study only a very small number of molecules or a small portion of the membrane surface. However, small measuring volumes mean week signals. Here comes the role of the surface plasmon enhanced field and evanescent mode inside the aperture. When the mode is close to its cut-off, the real part of its propagation constant along the axis of the hole tends to zero, which leads to a compression of the electromagnetic field at the entrance aperture, increasing even more the field density and thus the measured signal. In addition, as the field is evanescent inside the hole, the effective measuring volume does not extend to the entire hole depth (see Fig.1.12). The small cross-section of the holes reduces further on the measuring volume to much smaller values than permitted by the diffraction limit, in several cases volumes of the order of several attolitres have been reported.

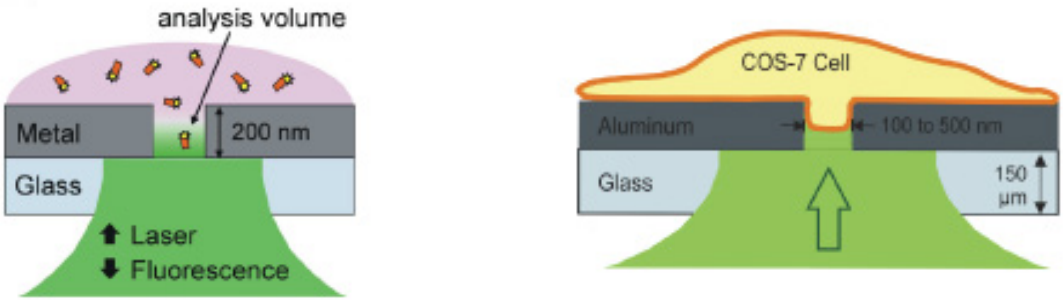

(a) (b)

Fig.1.12. Schematic presentation of (a) single-molecule fluorescence backside microscopy field density, and (b) tiny-portion cell membrane microscopy inside a metallic aperture (after [1.28] with the publisher's permission).

1.4.6. Non-resonant filters

Resonant filtering has its advantages, when narrow spectral bands are aimed, but in some important applications it is necessary to have wider bands, accompanied by angular and polarization invariance with respect to the incident wave. Such are the requirements for color filters used to separate the RGB colors on each pixel of the CCD cameras. A promising example [1.29] contains a small subwavelength grating consisting of circular metallic bumps with different diameters and heighst (Fig.1.13a) that can filter light in different spectral regions, depending on their geometrical parameters, (Fig.1.13b).

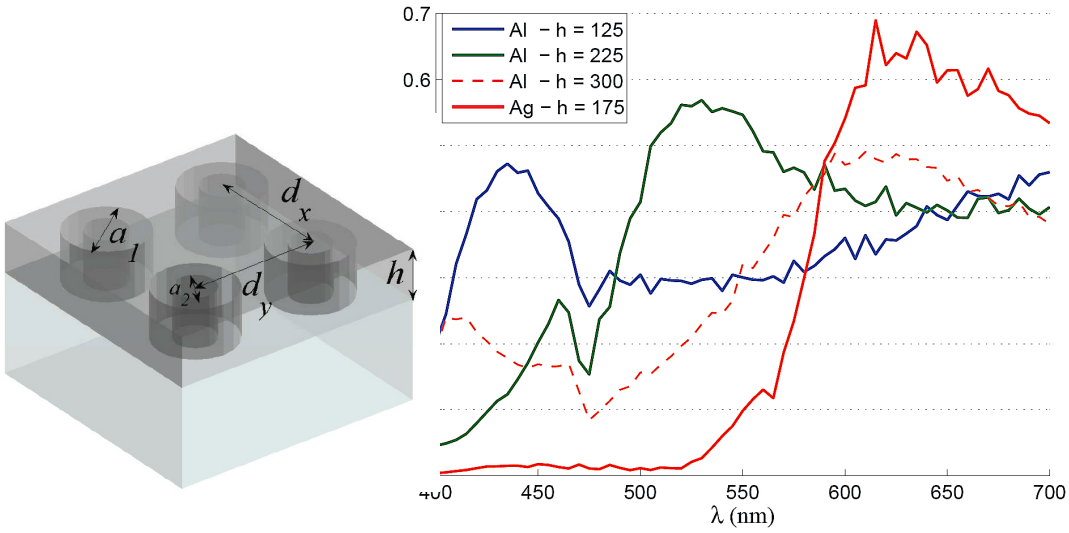

(a) (b)

Fig.1.13. (a) Nanostucture consisting of coaxial metallic cylinders, with a subwavelength period equal to 300 nm, external diameter 260 nm, and internal diameter 160 nm. (b) Transmission spectrum of the structure for different metals and cylinder heights, as shown in the inset (after [1.29] with the publisher's permission).

1.4.7. Flying natural gratings: butterflies, cicadas

The observation of Hopkinson (see Sec.1.1) of the diffraction on a handkerchief is far the less exotic grating that exists. As always, Nature had all the time to surpass humanity. A striking realization has been developed during the million-year long evolution of butterfly wings that

have so attractive coloring. The so called *Morpho rhetenor* butterflies have a non-pigment metallic blue color (*Fig.1.14*) that long has been attributed to multilayer reflection. However, Vukusic et al. [1.30] had the idea (and funds) to use an electron microscope to observe deeper in detail the structure of the scales, as reported in *Fig.1.15*a, a typical 3D structure that resembles a photonic crystal. The modeling with a 2D grating with a structure given in *Fig.1.15*b confirms the blue-spectrum reflection of the scales (*Fig.1.16*).

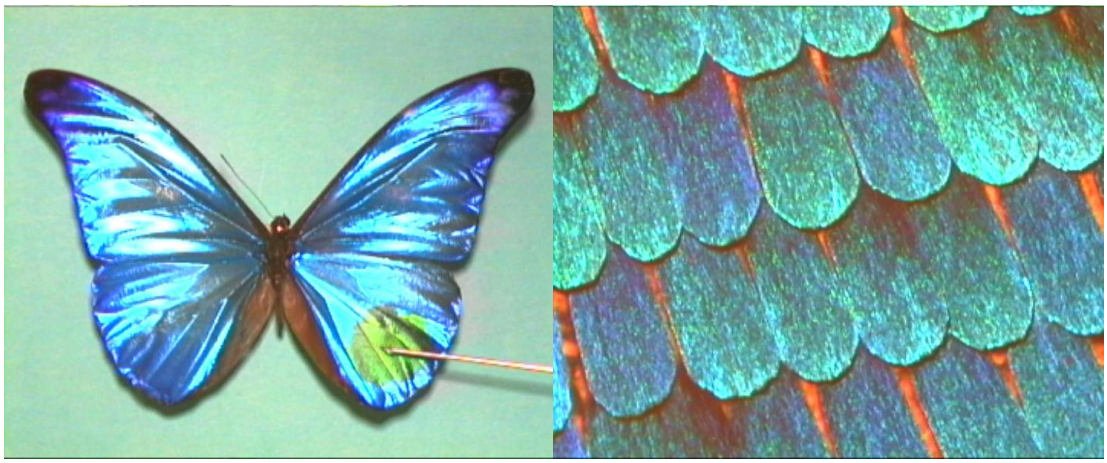

Fig.1.14. Entire view (to the left) and magnification of the scales (to the right) of a Morpho rhetenor butterfly (after [1.30] with the publisher's permission).

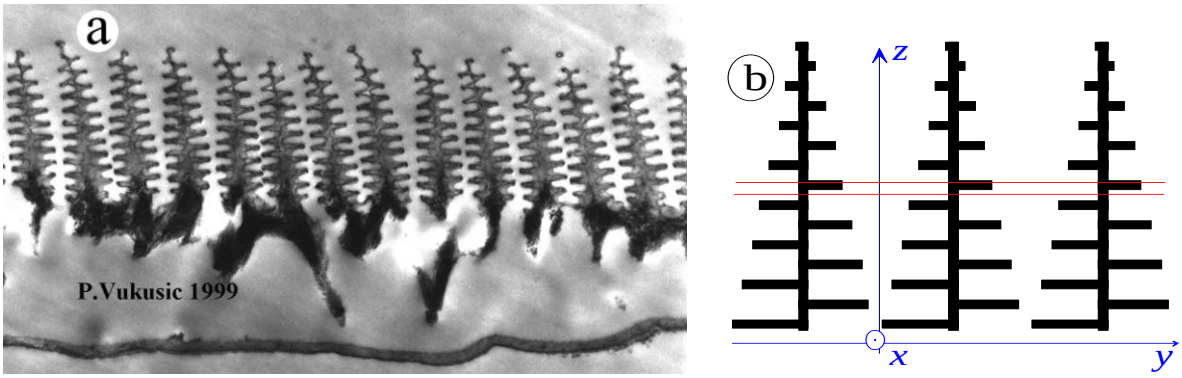

Fig.1.15. (a) Transmission electron microscope image showing the cross-section through a single Morpho rhetenor scale (after [1.30] with the publisher's permission). (b) Modeled structure; the two red lines define a grating layer, the optical index of white regions is 1 (after [1.31] with the publisher's permission).

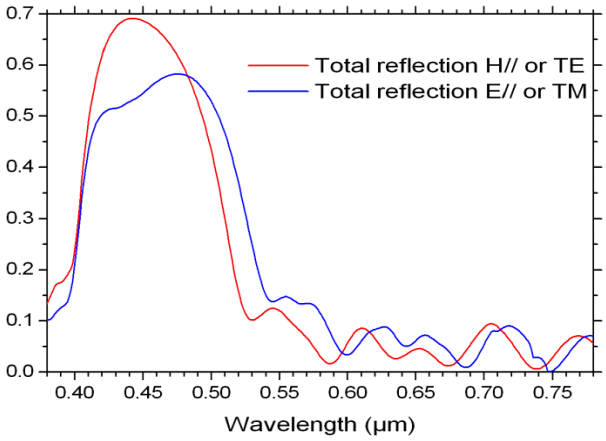

Fig.1.16. Spectral dependence of the reflection of the butterfly scale (after [1.31], with the publisher's permission).

Another "application" is used by the cicadas (quite common in the southern Europe, see Fig.1.17a) to camouflage themselves on the tree branches. Their wings are covered with an anti-reflection nanostructure, first observed by Xie et al. [1.32] and shown in Fig.1.17b. Anyone that has entered the microwave measuring rooms can identify the cones on the walls that are about 1 million times larger, as scaled to the wavelength.

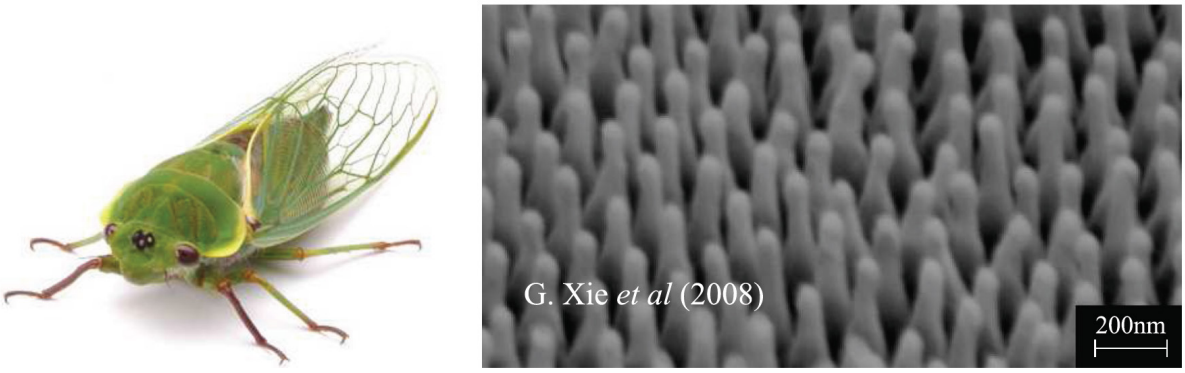

(a) (b)

Fig.1.17. (a) A photo of a cicada, and (b) the nanostructure pattern on its wings (after [1.32] with the publisher's permission).

1.5. Gratings in Integrated optics and plasmonic devices

Gratings are used in integrated optical devices to deviate the direction of propagation of waveguide modes and surface waves, for their focusing inside or outside the guide, or for energy transfer between different modes. Let us consider the case with one-dimensional periodicity. The grating equation can be applied not only to free-space waves, but to the waveguides modes. If the period is suitably chosen, it is possible to couple one mode to another:

$$\mathrm{Re}(k_{g,1}) = \mathrm{Re}(k_{g,2}) - K \tag{1.9}$$

where $k_{g,1}$ and $k_{g,2}$ are the propagation constants of the modes.

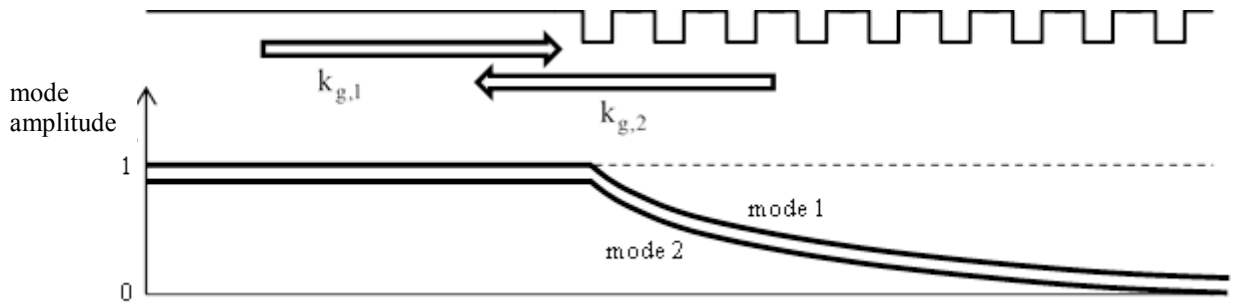

Fig.1.18. Upper part: schematical presentation of Bragg relief type lamellar grating deposited on a waveguide (dielectric or plasmonic) with two propagating modes. Lower part: energy carried by each mode.

It is possible to couple the mode propagating in a given direction to the same but contra-propagative mode. This is the case of the so-called Bragg gratings that act as a distributed mirror forming a forbidden zone for the mode propagation, in which the mode field decreases exponentially without being radiated in the cladding and in the substrate. The result is that it is rejected back into a contra-propagative direction (Fig.1.18). Due to the limit size of the grating region, a small part of the incident mode 1 is transmitted to the right, thus the reflected mode 2 carries smaller amount of energy. The grating grooves can be made curvilinear in order to focus the mode. The same effect can be obtained by replacing the 1D structure by 2D periodicity having also a period in the transversal y-direction (see Section 1.8).

1.6. Beam-splitting applications

The fact that the periodicity creates diffraction orders can be used to create multiple beams from a single laser beam. The most-commonly used device is symmetrical groove transmission gratings used as beam splitters for optical disk readers, where the wavelength of the laser source is constant. As a rule, the zero order beam reads the track and the two first order beams read adjacent tracks to keep the head both centered and focused. By controlling the groove depth, the ratio of zero to first orders transmission can be varied over a factor of 10, and a high degree of symmetry is inherent.

A special type of transmission grating can be used to generate an entire family of orders with a groove shape designed to make their intensities as equal as possible. This gives us multiple beam splitters, which may have 5 or even 20 orders on both sides of zero. A top view of such gratings under working conditions (with a laser input) gives rise to the term of "*fan-out gratings*". Applications are found in scanning reference planes for construction use, optical computing, and others [1.5, 33]. Such gratings tend to have large groove spacings (10 to 100 μm) and low depth modulations. The difficulty in making such gratings lies in achieving a groove shape that leads to a sufficient degree of efficiency uniformity among orders, especially if they are to function over a finite wavelength range. Two obvious candidates are cylindrical sections or an approximation of this shape in the form of a wide angle V with several segments of different angles. The choice may vary with the availability of the corresponding diamond tools. They have also been made by holographic methods, which are able to produce the parabolic groove form that gives the best energy uniformity

between the diffracted orders [1.34, 35]. Applications of fan-out gratings are found in scanning reference planes for construction use, in biophysics for simultaneous treatment of great number of samples, etc.

By combining two such grating at right angles to each other, an accurately defined 2D array of laser beams is generated to be used for calibrating the image field distortion of large precision lenses, in robotic vision systems, or in parallel optical computing. Instead of using two 1D periodical grating, it is possible to use a single large-period 2D crossed grating with specially optimized pattern inside each period [1.36].

1.7. Subwavelength gratings for photovoltaic applications

As explained in Sec.1.4, resonant excitation in metallic gratings can lead to a total absorption of incident light, effect necessary for the efficient work of photovoltaic devices. The problem with surface plasmon excitation and the accompanying light absorption is that its wave is not localized, thus it is characterized by a well-determined value of propagation constant along the surface, because non-local effects in the real space are localized in the inverse space. This is why the surface plasmon anomalies have very narrow angular and spectral width, an advantage in detector construction, but failing in photovoltaics. Evidently, effects that are less localized in the inverse space will be more localized in the real space. This leads us to cavity resonances, volume plasmonic excitation, and surface plasmons that propagate in the vertical direction but are localized in x-y direction. Cavity resonances in deep grooves or in closed cavities, like embedded dielectric spheres or cylinders inside a metallic sheet can absorb light within relatively large angular region (20-30 deg) [1.37-40].

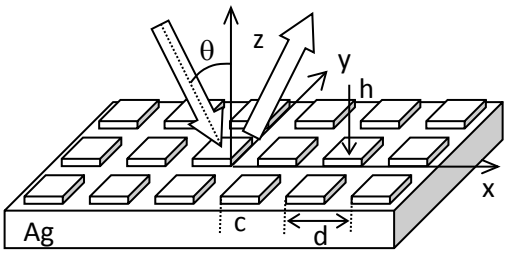

Fig.1.19. Crossed metallic diffraction grating

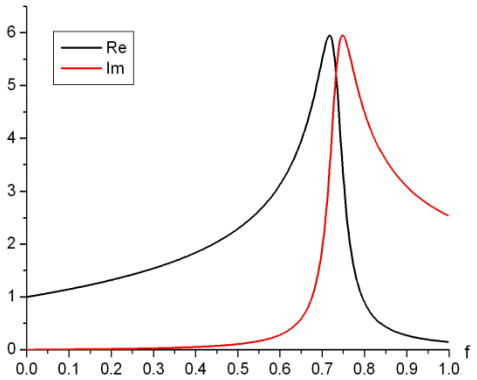

Fig.1.20. Real and imaginary part of the effective refractive index of the structure of Fig.1.19 as a function of the filling ratio when the period is much shorter than the wavelength λ = 457 nm.

However, the problem of cavity resonances is that they are strongly wavelength-sensitive. An alternative approach consists of using metamaterial behavior of small-feature structures. By mixing metallic and dielectric materials one can, in general, obtain strongly absorbing alloys with effective refractive index that does not exist for known materials. In addition, the equivalent metamaterial layer has a uniaxial anisotropy with axis perpendicular to the grating plane. Thus inside the xOy plane it has isotropic properties and its response is polarizationally independent, at least close to normal incidence.

For example, a crossed channel grating as presented in Fig.1.19 and made of silver bumps on a silver substrate. It can strongly absorb the incident light in much larger spectral

domain when compared with the surface plasmon excitation effects. As can be observed in Fig.1.20, close to a filling ratio ($f = c^2/d^2$) equal to 0.7, both the real and the imaginary part of the effective refractive index for small-period structure grow significantly to values that no existing material has in this spectral domain. This increases the effective optical thickness of the system, together with its absorption, so that a very thin grating ($h < 10$ nm) can totally absorbed incident light [1.41]. Because of the 2D periodicity of the structure, it becomes polarization insensible. Moreover, this effect has no resonant nature and is extended angularly to almost the entire set of angles of incidence, as seen in Fig.1.21. In addition, the spectral domain of absorption stronger than 75% extends to a more than 100 nm interval [1.42].

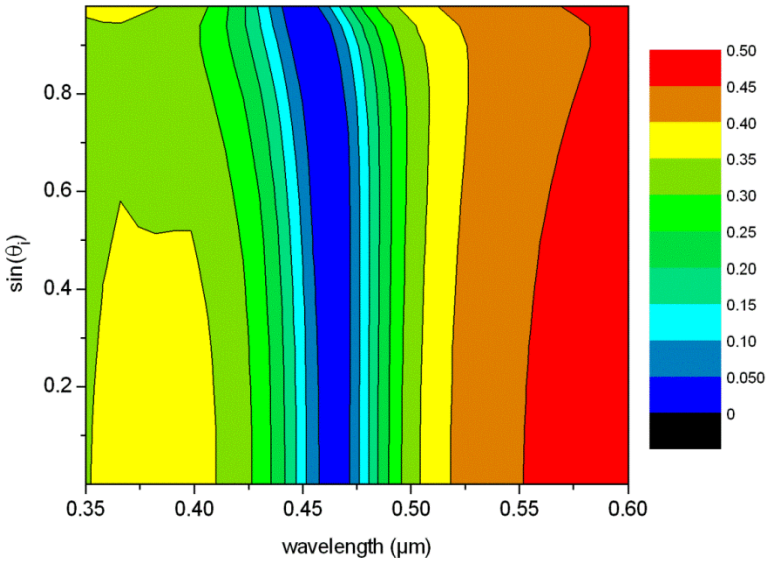

Fig.1.21. Reflectivity of the crossed graing in Fig.1.19 as a function of the wavelength and of the sine of the incident angle. Period d = 3 nm, system thickness h = 6.2 nm, filling factor = 0.7, i.e. c/d = 0.837.

However, the use of such structures for practical applications requires not only a larger spectrum of strong absorption, but also needs that the absorbed light is not immediately transformed into heat and that it is kept inside the photovoltaic layer that transforms light into electricity. The simple structure represented in Fig.1.19 is not sufficient to efficiently fulfill these purposes. It has to be complicated by a structuring in the depth of the device (Fig.1.22). Light is incident from the top of the device. Its entering part (in blue) is designed to act as an antireflector, and absorbs most of the blue part of the spectrum. The green part is absorbed in the middle of the rods, while the back-side part (in red) absorbs the longer wavelengths, and serves as a reflector to prevent the unabsorbed part to be lost in the substrate [1.43].

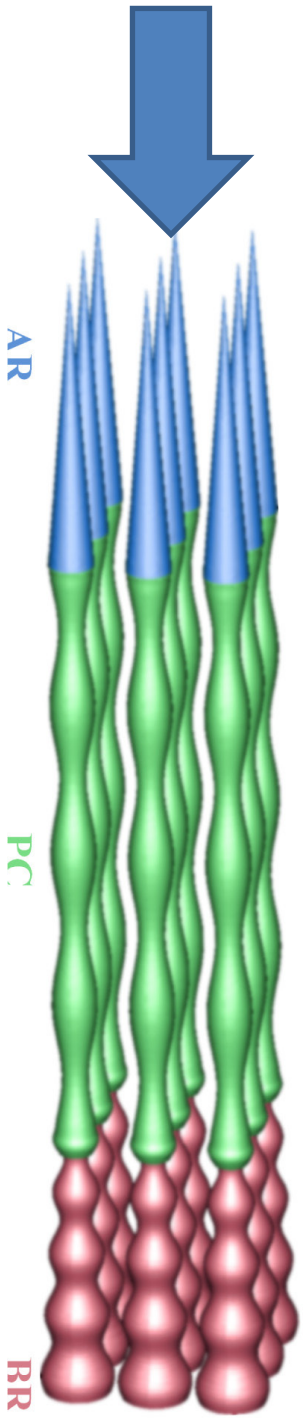

Fig.1.22. Grating rods as optimal photovoltaic absorber (after [1.43], with the publisher's permission)

1.8. Photonic crystals

Periodic structures in optics can serve for the photons in the same manner as semiconductor crystals for electrons. This common feature led in the '90s to call such structures *photonic crystals*. As discovered by Yablonovich [1.44, 45], they present band-gaps that forbid propagation and thus guaranteeing 100% reflection inside the band. While this property is widely known and largely used in multilayer dielectric mirrors (Fig.1.23a), the band gap of 1D photonic crystals is limited in relatively smaller angular interval. Some other structures that have 2D periodicity combined with a nanostructuring in the third dimensions can be found in Figs.1.15, 17, and 22.

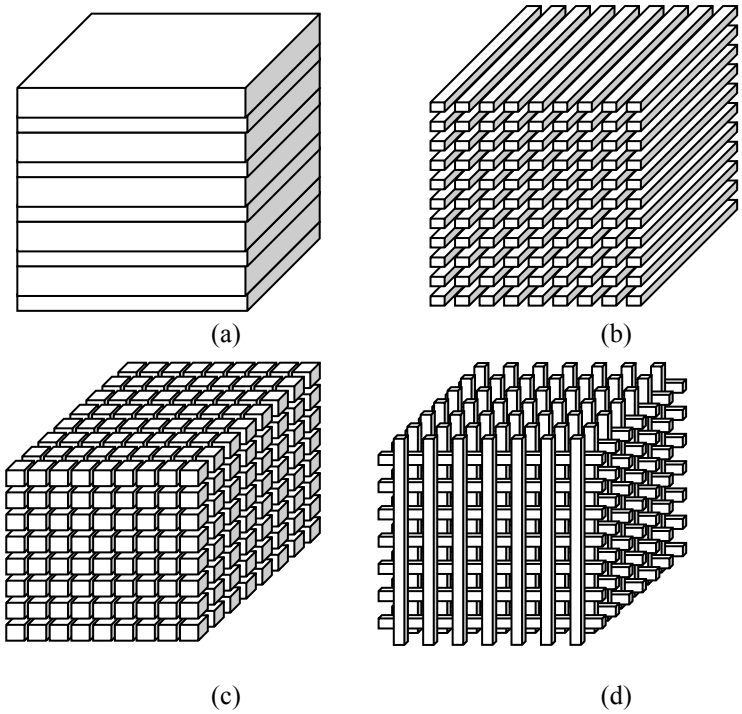

Fig.1.23. Schematic representation of (a) one-, (b) two- and (c, d) three-dimensional photonic crystals.

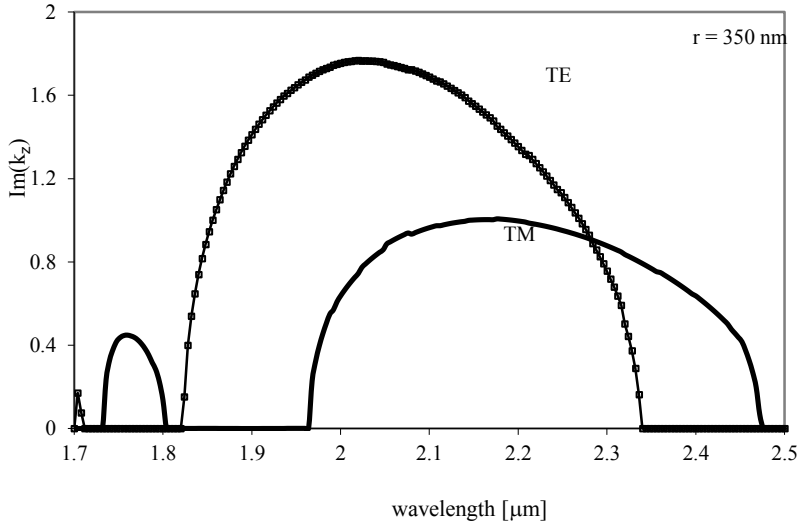

Fig.1.24. Forbidden bands for the photonic crystalmade of circular cylinders with d = 1.414 μm, r = 0.35 μm (after [1.46] with the publisher's permission).

A typical band-gap structure of a 2D photonic crystal presented in Fig.1.23b, but its surface cut at an angle of 45° with respect to the vertical direction, is given in Fig.1.24 for a system having period d = 1.414 μm in both directions, and consists of circular cylindrical rods with radius equal to 0.35 μm and optical index of 2.9833 in air as a matrix. The figure presents the values of the smallest imaginary part of k_z. As can be seen, a forbidden gap in both TE and TM polarization exists for $\lambda \in [1.97, 2.33\,\mu m]$ [1.46, 47]. Inside the band gap electromagnetic field intensity diminishes exponentially and the entire incident light is reflected back. However, the choice of the ratio of the wavelength and the period allows for the propagation of the -1st order in reflection. This gives the possibility to guide the entire incident light into this order, thus perfect blazing in the -1st diffracted order can be obtained in both polarizations, a property that is strongly desirable in many applications. And indeed, Fig.1.25 presents the diffraction efficiency of the system having cylinders with radii of 350 nm (a) and 150 nm (b). A well-defined spectral region with almost 100% efficiency in unpolarized light can be observed.

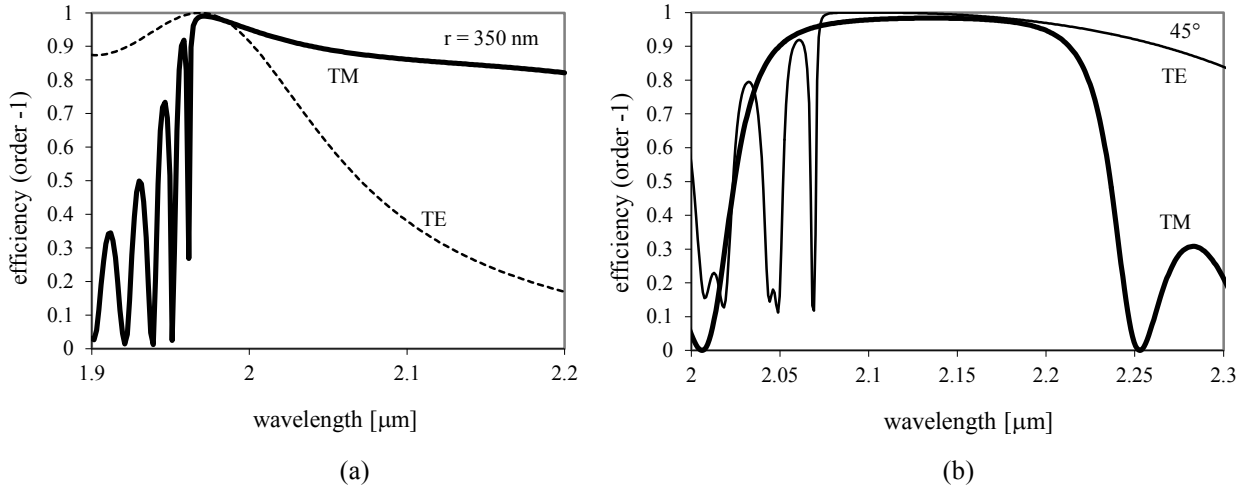

Fig.1.25. Diffraction efficiency in order -1 as a function of the wavelength lying inside the band gap. (a) r = 350 nm, (b) r = 150 nm (after [1.46] with the publisher's permission).

The property of totally reflecting the incident light whatever the direction, can be of great importance for light guiding and manipulation. Light confinement and guiding in a single dimension is ensured by using planar waveguides. Channel waveguides and optical fibers confine light in two dimensions, but they suffer from two important limitations: dispersion and bending losses. High bending angles damage the guiding properties and lead to radiation losses. A waveguide constructed with photonic crystal walls can ensure bending, Fig.1.26, without losses even at 90°, as predicted numerically [1.48].

It is impossible even only to list here the *potential* applications of photonic crystal devices, as for example negative refraction, perfect lenses construction, photonic crystal fibers, nonlinear optical applications. The main problem that persists is purely *technological*: while it is relatively easy to fabricate 3D periodically structures working in the microwave and far-IR domain, scaling down to the visible and the near-IR presents a lot of challenges to optical industry. Fortunately, the process of fiber manufacturing enables literally such mechanical scaling of the dimension, transferring the initial large-diameter preform into a thin fiber by pulling it. If the preform is carefully drilled with macroscopic holes, they are preserved in the final fibers, but scaled to nanodimensions.

In the resulting photonic crystal fiber (Fig.1.27), light is preserved in the central hollow guide by repulsion from the surrounding structure that presents a forbidden gap for the working wavelength.

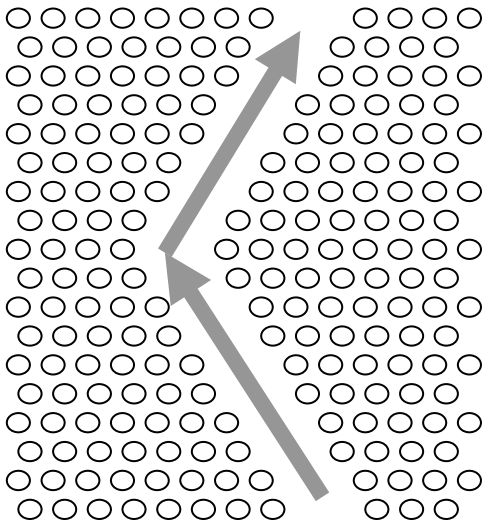

Fig.1.26. Light guiding in a cavity formed by photonic crystal walls consisting of cylindrical objects

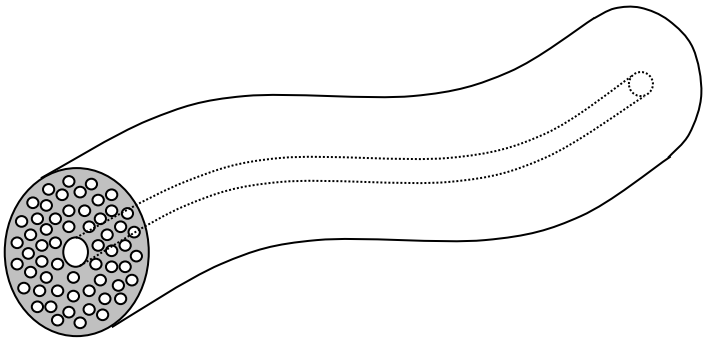

Fig.1.27. Schematic representation of a portion of an optical fiber – photonic crystal hybrid structure. Small cylindrical holes run along the fiber length. A central hole (shown with a dashed line inside the fiber) serves as an energy propagator, which ensured low dispersion, low absorption losses and high damage threshold

1.9. References:

1. *The Concise Oxford Dictionary of English Etymology in English Language Reference* accessed via Oxford Reference Online
2. D. Rittenhouse "An optical problem proposed by F. Hopkinson and solved," J. Am. Phil. Soc. **201**, 202-206 (1786)
3. T. Young: "On the theory of light and colors," Phil. Trans. **II**, 399-408 (1803)
4. J. Fraunhofer: "Kurtzer Bericht von the Resultaten neuerer Versuche über die Gesetze des Lichtes, und die Theorie derselbem," Gilberts Ann. Phys. **74**, 337-378 (1823); "Über die Brechbarkeit des electrishen Lichts," K. Acad. d. Wiss. zu München, April-June 1824, pp.61-62
5. E. Loewen and E. Popov, : *Diffraction Gratings and Applications*, (Marcel Dekker, New York, 1997)
6. J. Hoose and E. Popov, "Two-dimensional gratings for low polarization dependent wavelength demultimlexing," Appl. Opt. **47**, 4574 – 4578 (2008)
7. E. Popov, J. Hoose, B. Frankel, C. Keast, M. Fritze, T.Y. Fan, D. Yost, and S. Rabe: "Diffraction-grating based wavelength demultimlexer," Opt. Expr. 12, 269-275 (2004)
8. J. Hoose, R. Frankel, E. Popov, and M. Nevière: "Grating device with high diffraction efficiency," US patent No 6958859/25.10.2005
9. E. Popov, B. Bozhkov, D. Maystre, and J. Hoose: "Integral method for echelles covered with lossless or absorbing thin dielectric layers," Appl. Opt. **38**, 47-55 (1999)
10. H. U. Käufl, "N-band long slit grism spectroscopy with TIMMI at the 3.6 m telescope," The ESO Messenger, **78**, 4 -7 (Dec. 1994)
11. K. Knop, "Diffraction gratings for color filtering in the zero diffracted order," Appl. Opt. **17**, 3598 – 3603 (1978)
12. Lord Rayleigh, "Note on the Remarkable Case of Diffraction Spectra Described by Prof. Wood," Philos. Mag. **14**, 60 (1907)
13. R. W. Wood, "On a remarkable case of uneven distribution of light in a diffraction grating spectrum," Phylos. Mag. **4**, 396-402 (1902)
14. U. Fano, "The theory of anomalous diffraction gratings and of quasi-stationary waves on metallic surfaces (Sommerfeld's waves)," J. Opt. Soc. Am. **31**, 213-222 (1941)
15. A. Hessel and A. A. Oliner, "A new theory of Wood's anomalies on optical gratings," Appl. Opt. **4**, 1275-1297 (1965)
16. M. C. Hutley and D. Maystre, "Total absorption of light by a diffraction grating," Opt. Commun. **19**, 431-436 (1976)
17. M. J. Jory, P. S. Vukusic, and J. R. Sambles, "Development of a prototype gas sensor using surface plasmon resonance on gratings," Sens. Actuators B **17,** 203-209 (1994)
18. N. Bonod, E. Popov, and R. C. McPhedran, "Increased surface plasmon resonance sensitivity with the use of double Fourier harmonic gratings," Opt. Express **16**, 11691-11702 (2008)
19. L. Mashev and E. Popov: "Zero Order Anomaly of Dielectric Coated Grating," Opt. Commun. **55**, 377 (1985)
20. G. A. Golubenko, A. S. Svakhin, V. A. Sychugov, A. V. Tischenko, E. Popov and L. Mashev: "Diffraction Characteristics of Planar Corrugated Waveguides," J. Opt. Quant. Electr. **18**, 123 (1986)
21. E. Popov, L. Mashev and D. Maystre: "Theoretical Study of the Anomalies of Coated Dielectric Gratings," Opt. Acta **33**, 607 (1986)
22. S. Wang, R. Magnusson, J. Bagdy, and M. Moharam, "Guided-mode resonances in planar dielectric-layer diffraction gratings," J. Opt. Soc. A **7**, 1470-1474 (1990)
23. S. Tibuleac and R. Magnusson, "Narrow-linewidth bandpass filters with diffractive thin-film layers," Opt. Lett. **26**, 584-586 (2001)

24. A. Sentenac and A.-L. Fehrembach, "Angular tolerant resonant grating filters under oblique incidence," J. Opt. Soc. Am. A, **22**, 475-480 (2005)
25. T. W. Ebbesen, H. J. Lezec, H. F. Ghaemi, T. Thio, P. A. Wolff, "Extraordinary optical transmission through subwavelength hole arrays", Nature, **391**, 667-669 (1998)
26. E. Popov, M. Neviere, S. Enoch, and R. Reinisch, "Theory of light transmission through subwavelength periodic hole arrays," Phys. Rev. B, **62**, 16100-16108 (2000)
27. S. Enoch, E.Popov, M.Nevière, and R. Reinisch, "Enhanced light transmission by hole arrays," J. Opt. A: Pure Appl. Opt. **4**, S83-S87 (2002)
28. J. Wenger, D. Gerard, P.-F. Lenne, H. Rigneault, N. Bonod, E. Popov, D. Marguet, C. Nelep, T. Ebbesen, "Biophotonics applications of nanometric apertures," Int. J. Materials and Product Technology. **34**, 488-506 (2009)
29. G. Demésy, "Modélisation électromagnétique tri-dimensionnelle de réseaux complexes. Application au filtrage spectral dans les imageurs CMOS", Ph. D. Thèse 2009AIX300006, Univ. Aix-Marseille III, Marseille (2009)
30. P. Vukusic, J.R. Sambles, C.R. Lawrence and R.J. Wootton, "Quantified interference and diffraction in single *Morpho* butterfly scales,"Proceedings: Biological Sciences, The Royal Society of London **266**, 1403 -1411 (1999)
31. B. Gralak, G. Tayeb, and S. Enoch, "Morpho butterflies wings color modeled with lamellar grating theory," Opt. Express **9**, 567-578 (2001)
32. G. Xie, G. Zhang, F. Lin, J. Zhang, Z. Liu, and S. Mu, "The fabrication of subwavelength anti-reflective nanostructures using a bio-template," *IOP Nano*, **19**, 95605, (2008)
33. L. P. Boivin: "Multiple imaging using various types of simple phase gratings," Appl. Opt., **11**, 1782–1792 (1972).
34. P. Langlois and R. Beaulieu, "Phase relief gratings with conic section profile in the production of multiple beams," Appl. Opt. **29**, 3434-3439 (1990).
35. D. Shin and R. Magnusson: "Diffraction of surface relief gratings with conic cross–sectional gratings shapes," J. Opt. Soc. Am. A **6**, 1249–1253 (1989).
36. NOI Bulletin, v.**5**, no.2, July 1994, Québec, Canada
37. N. Bonod and E. Popov, "Total light absorption in a wide range of incidence by nanostructured metals without plasmons," Opt. Lett. **33**, 2287-2289 (2008)
38. E. Popov, L. Tsonev, and D. Maystre, 'Lamellar metallic grating anomalies," Appl. Opt. **33**, 5214-5219 (1994)
39. E. Popov, N. Bonod, and S. Enoch, "Comparison of plasmon surface wave on shallow and deep 1D and 2D gratings," Opt. Express **15**, 4224-4237 (2007)
40. E. Popov, D. Maystre, R. C. McPhedran, M. Nevière, M. C. Hutley, and G. H. Derrick, "Total absorption of unpolarized light by crossed gratings," Opt. Express **16**, 6146-6155 (2008)
41. J. Le Perchec, P. Quémerais, A. Barbara, and T. López-Rios, "Why metallic surfaces with grooves a few nanometers deep and wide may strongly absorb visible light," Phys. Rev. Lett. **100**, 066408 (2008)
42. E. Popov, S Enoch, and N. Bonod, "Absorption of light by extremely shallow metallic gratings: metamaterials behavior," Opt. Express **17**, 6770-6781 (2009)
43. G. Demésy and S. John, "Solar energy trapping with modulated silicon nanowire photonic crystal," J. Appl. Phys., 074326 (2012)
44. E. Yablonovitch, "Inhibited spontaneous emission in solid-state physics and electronics," Phys. Rev. Lett. **58**, 2059-2062 (1987)
45. E. Yablonovitch, "Photonic crystals," J. Modern Opt., **41**,173-194 (1994)
46. E. Popov, B. Bozhkov, and M. Nevière, "Almost perfect blazing by photonic crystal rod gratings," Appl. Opt. **40**, 2417-2422 (2001)

47. E. Popov and B. Bozhkov: "Differential method applied for photonic crystals", Appl. Opt. **39**, 4926 (2000)
48. G. Tayeb and D. Maystre, "Rigorous theoretical study of finite size two-dimensional photonic crystals doped by microcavities," J. Opt. Soc. Am. A **14**, 3323-3332 (1997)